ELSEVIER

Polymer 43 (2002) 3979–3986

polymer

www.elsevier.com/locate/polymer

Morphology and mechanical properties of semi-interpenetrating polymer networks from polyurethane and benzyl konjac glucomannan

Yongshang Lu, Lina Zhang*

Department of Chemistry, Wuhan University, Wuhan 430072, People's Republic of China

Received 19 December 2001; received in revised form 4 March 2002; accepted 6 March 2002

Abstract

A series of semi-interpenetrating polymer network (semi-IPN) films coded as UB from castor oil-based polyurethane (PU) and benzyl konjac glucomannan (B-KGM) were prepared, and they have good or certain miscibility over entire composition range. Morphology, miscibility and properties of the UB films were investigated by using scanning electron microscopy (SEM), differential scanning calorimetry, dynamic mechanical analysis, ultraviolet spectrometer, wide-angle X-ray diffraction and tensile test. The results indicated that the UB films exhibited good miscibility when B-KGM content was lower than 15 wt%, resulting in relatively high light transmittance, breaking elongation and density. With an increase of the B-KGM content from 20 to 80 wt%, a certain degree of phase separation between PU and B-KGM occurred in the UB films. The tensile strength of the films UB increased from 7 to 45 MPa with an increase of B-KGM content from 0 to 80 wt%. By extracting the B-KGM with *N*, *N*-dimethylformamide from the semi-IPN, the morphology and phase domain size of the UB films were clearly observed by SEM. A continuous phase and dual-continuous phase model describing the semi-IPN were proposed to illustrate the morphology and its transition.

Keywords: Semi-interpenetrating polymer networks; Polyurethane; Konjac glucomannan

1. Introduction

Few scientific endeavors in human history have had a greater impact on mankind than those concentrated in polymer science arena, and the polymer science and technologies in the 21st century are facing new challenges and opportunities [1]. Environmental friendly materials from renewable resources, such as cellulose, polysaccharides, protein, etc. are worthy targets for further innovation as we move. Konjac glucomannan (KGM), a low cost polysaccharide obtained from the tubers of the *Amorphophallus konjac* plants, is a linear random copolymer of (1→4) linked β-D-mannose and β-D-glucose units in a molar ratio of 1.6:1 with a low degree of acetyl groups at C-6 position [2]. It is noted that facilitating hydrogen bonding formation of excessive hydroxyl groups in KGM with other polymers results in gelation or enhances miscibility in binary system of KGM with other polymers [3]. Moreover, its characters of richness, water-soluble and easiness to be derivatived entitle KGM to be a novel polymer material applied in the fields of coating, packing and medical [4–7]. Thus, it is interesting to use the KGM to prepare biodegradable water-resistant materials by modifying with physico-chemical methods.

Interpenetrating polymer networks (IPNs) are defined as a combination of two polymers in network form, at least one of which is cross-linked in the immediate presence of the other [8]. The IPNs have gained widespread acceptance recently in applications as damping materials [9], biomedical materials [10], gas transport membrane [11], and electrical/electronic devices [12]. Polyurethane (PU), a class of very useful and versatile material, has been widely used as the individual polymer possessing networks structure in view of its good flexibility and elasticity or as component of IPNs. In our laboratory, the grafted and semi-IPN materials derived from castor oil-based PU with natural products, such as nitrocellulose [13], nitrochitosan [14] and nitrokonjac glucomannan [4], have been successfully prepared. It indicates that introduction of the natural polymers into PU plays an important role in accelerating cure and in enhancing biodegradability. The biodegradation test of cellulose films coated with these PU/natural polymer IPNs has indicated that the microorganisms directly attacked the water-resistant coating layer and then penetrated into the cellulose to speedily metabolize, accompanying with producing CO_2, H_2O, glucose cleaved from cellulose, and

* Corresponding author. Tel.: +86-27-8721-9274; fax: +86-27-8788-2661.

E-mail address: lnzhang@public.wh.hb.cn (L. Zhang).

0032-3861/02/$ - see front matter
PII: S0032-3861(02)00206-9

aromatic ethers molecules decomposed from the PU coating [15]. However, the content of natural polymers in these IPN materials was lower than 40 wt%, otherwise phase separation between two polymers appeared, resulting in the preparation difficulty or the poor mechanical properties of the materials. An increasing of natural polymer content in the IPN systems is essential for the successful utilization of the renewable resources and improvement of biodegradability. Particularly, a clear determination of the phase domain size and shape is important to know the morphology of multi-component polymer system [16].

In this work, we attempted to prepare a benzyl KGM (B-KGM), whose hydrophobic benzyl groups should be more compatible with soft segments of castor oil-based PU, and then to obtain the IPNs by reacting the B-KGM having content from 0 to 80 wt% with the castor oil-based PU prepolymer. In this case, the B-KGM as a linear macromolecule can be interpenetrated into the PU networks to form a semi-IPN structure. The morphology, miscibility, and properties of the PU/B-KGM semi-IPN films were investigated in relation to the B-KGM content. Further, the phase domain size and phase continuity of the polymer components were discussed.

2. Experimental

2.1. Preparation of benzyl konjac glucomannan

All the chemical reagents used were obtained from commercial sources in China. Purified KGM was supplied by Zhuxi Konjac Institute of China. The castor oil was dehydrated at 100 °C under 20 mmHg for 1 h. 2,4-Toluene diisocyanate was redistilled before use. *N*, *N*-dimethylformamide (DMF) was dried over molecular sieves. Five grams of KGM and 0.1 g of tetramethylammonium iodide were dissolved in 200 ml water, and then were introduced to a three-necked flask equipped with a mechanical stirrer, dropping funnel and condenser. The flask was placed in an oil bath at 40 °C and stirred vigorously, while 50 g of 40 wt% sodium hydroxide aqueous solution was added dropwise. The resulting alkali-KGM slurry was stirred at 40 °C for 1 h before adding dropwise 15 g of benzyl chloride. The reaction was performed at 100 °C for 2 h to obtain the slightly yellow product as a precipitate. The precipitate was distilled with water-vapor, extracted with ethanol, and then washed with ether and water, finally vacuum-dried at room temperature to obtain a white powder of the B-KGM. Fourier transform infrared (FT-IR) spectrum of the B-KGM film prepared from its DMF solution exhibited characteristic absorption at 3030 cm^{-1} (C–H aromatic stretching), 2959, 2873 cm^{-1} (CH_2 stretching), 1607, 1586 cm^{-1} (C–C aromatic stretching), 1497, 1454 cm^{-1} (C–H aromatic in-plane deformation) and 738, 698 cm^{-1} (C–H aromatic out of plane deformation). ^{1}H NMR spectrum of B-KGM was recorded on a DRX-400BB spectrometer (Bruker Co., Germany, Switzerland) in DMSO-d_6 at room temperature and the B-KGM concentration was adjusted to 5 wt%. The ^{1}H NMR spectrum of the B-KGM is shown in Fig. 1. The main peaks appeared at 7.24 ppm (H of phenyl), 3.31, 3.34 ppm (H of methylene in benzyl), indicating an occurrence of the substitution. The degree of substitution (DS) was calculated to be 1.2 from elemental data obtained by using an elemental analyzer (CHN-O-RAPID Heraeus Co., Germany) according to Ref. [17]. The weight average molecular weight (M_w) of B-KGM in dimethylsulfoxide (DMSO) was determined to be 3.1×10^5 with Debye plots by using a multi-angle laser photometer equipped with a He–Ne laser ($\lambda = 633$ nm; DAWN-DSP, Wyatt Technology Co., USA), and Astra software was utilized for the data acquisition and analysis.

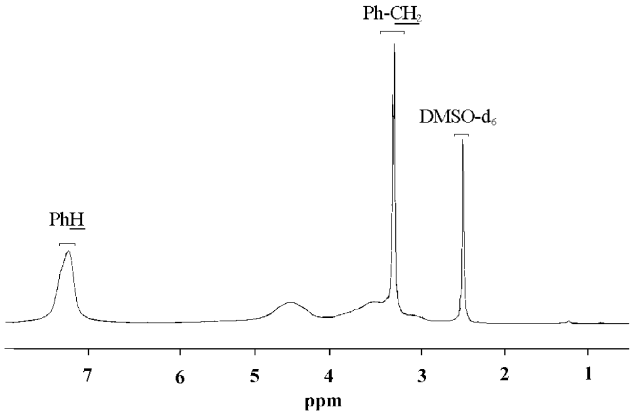

Fig. 1. The ^{1}H NMR spectrum of the B-KGM.

2.2. Preparation of polyurethane/B-KGM films

The castor oil-based PU prepolymer (NCO/OH = 2) was prepared according to the method described by Sperling [18]. Three grams of PU prepolymer was mixed with B-KGM of desired mass and 1,4-butanediol as chain extender (the amount being adjusted to give total NCO/OH = 1) in DMF at room temperature. The resulting reactant solution was given a solid content of about 20 wt%, and then poured into a mold. The casting solutions were cured at room temperature for 30 min and then heated at 60 °C for 4 h except for the one without B-KGM for 10 h to form dried films with thickness of 150 μm. The PU/B-KGM films were coded as UB-5, UB-10, UB-15, UB-20, UB-30, UB-40, UB-50, UB-60 and UB-80, respectively, corresponding to the B-KGM content of 5, 10, 15, 20, 30, 40, 50, 60 and 80 wt% in the films. The films from pure PU and B-KGM were coded as PU and B-KGM, respectively. The samples were vacuum-dried at room temperature for 2–3 days before characterization.

2.3. Characterization

Attenuated total reflection infrared spectroscopy was performed on a spectrometer (1600, Perkin–Elmer Co.,

USA). The samples were taken at random from flat films and the data were collected over 16 scans with a resolution of 4 cm^{-1} at room temperature.

The density of the films PU and UB was measured at 25 °C by determining the weight of a volume-calibrated pycnometer filled with a mixture of NaCl aqueous solution and ethanol, in which the samples achieved floatation level. The density of the sample equals the mixture density.

To study the networks structure and intermolecular interaction between PU and B-KGM, the extraction of the UB films was performed as following: 0.3 g UB film enclosed in a nylon mesh was immerged in DMF accompanying mild stirring for 30 h at room temperature, thus the B-KGM and uncross-linked PU were dissolved to remove from the PU networks during extraction process. The extracted UB films were vacuum-dried at room temperature and weighted. The percentage extracted amount was calculated by

$$\text{extracted amount}(\%) = \frac{W_i - W_e}{W_i} \times 100\%$$

where W_i and W_e are weight of initial and extracted UB films, respectively. The extracted UB films were frozen in liquid nitrogen and fractured immediately, and the morphology of fractured sections of the UB films were observed and photographed by using a scanning electron microscopy (SEM; S-570, Hitachi, Japan) after being coated with gold.

Differential scanning calorimetry (DSC) was carried out on a thermal analyzer (DSC-2C, Perkin–Elmer Co., USA) in the temperature range from −50 to 200 °C with a heating rate of 10 °C/min, and the sample weight was 17 ± 3 mg. Dynamic mechanical analysis (DMA) was performed with a dynamic mechanical thermal analyzer (DMTA-IV, Rheometric Scientific Co., USA) at 1 Hz and a heating rate of 5 °C/min in the temperature range from −50 to 200 °C. The specimens with typical size of 10 mm × 10 mm (length × width) were used here.

Wide-angle X-ray diffraction patterns were recorded on an X-ray diffractometer (D/MAX-1200, Rigaku Denki, Japan) in the range of $2\theta = 4 - 40°$ with Cu kα radiation ($\lambda = 1.5406 \times 10^{-10}$ m) at 40 kV and 30 mA. The percent light transmittance of the films with thickness of 150 μm was measured by using an ultraviolet spectrophotometer (UV-160A, Shimadzu, Japan).

The tensile strength (σ_b) and breaking elongation (ε_b) of the films were measured on a universal testing machine (CMT-6503, Shenzhen SANS Test Machine Co. Ltd, China) according to the ISO6239-1986 standard with a rate of 50 mm/min.

3. Results and discussion

3.1. Miscibility of the UB films

The interactions between chemical groups on either the same or different molecules can cause a shift of the IR peak position of the participating groups. The interactions are commonly observed in macromolecules systems by existence of hydrogen bonds, which can promote phase mixing [19,20]. IR spectra of the PU and UB films are shown in Fig. 2. The PU displayed characteristic peaks at about 1724 and 1703 cm^{-1}, which were assigned to the absorption of free carbonyl stretching and hydrogen bonded carbonyl stretching with NH groups, respectively [19,20]. Intensity of peak located at 1703 cm^{-1} decreased, while that of peak at 1724 cm^{-1} increased gradually for the UB films with an increase of B-KGM content, implying that hydrogen bonded hard segment in the UB films decreased. Moreover, the hydrogen bonded NH stretching absorption of PU at 3318 cm^{-1} for the UB films slightly shifted to higher wavenumber, indicating an enhancement of free NH group fraction in the UB films [19–21]. This implies that the original inter- and intra-molecular hydrogen bonds involved in PU films were destroyed due to the interpenetration and entanglements between PU and B-KGM.

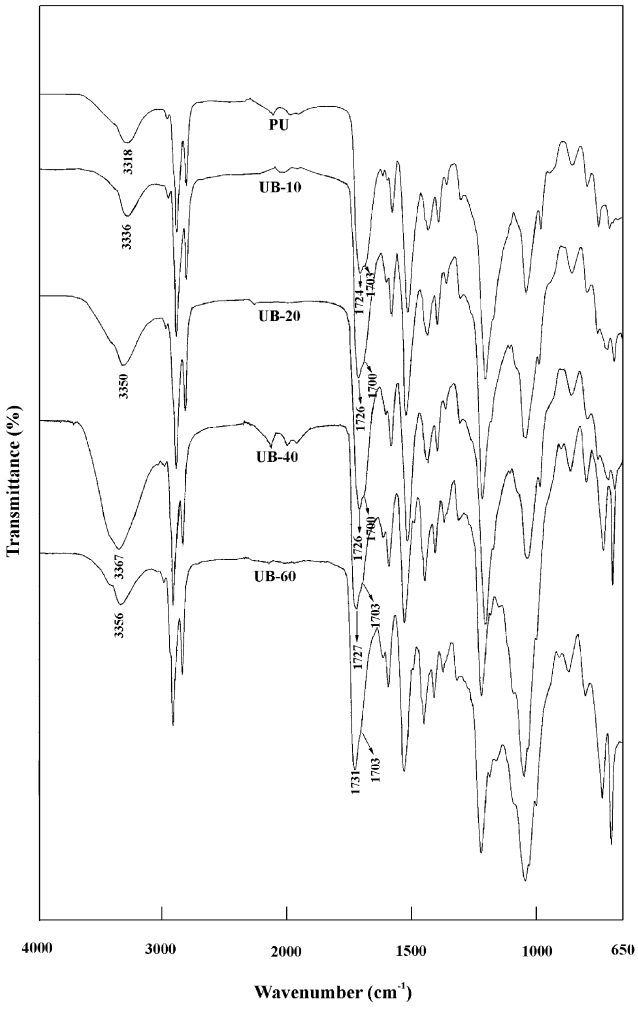

Fig. 2. The FT-IR spectra of films PU and UB.

The measured density and the density calculated from the volume additivity of the components as a function of

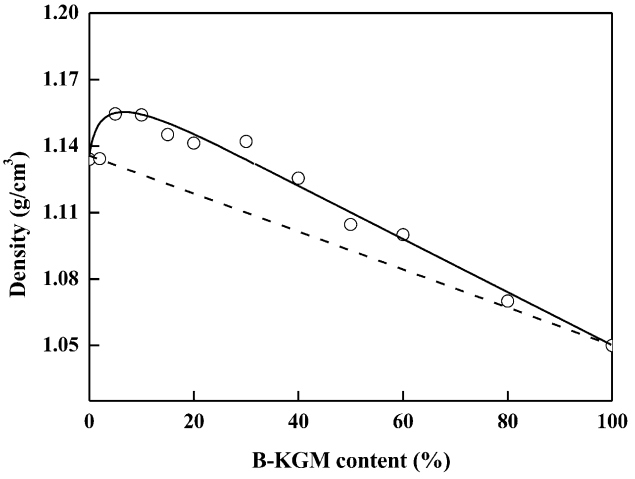

Fig. 3. B-KGM content dependence of the densities from experimental (○) and additivity rule (- - -) for the films PU, B-KGM and UB.

B-KGM content are shown in Fig. 3. If IPN system was composed of a rubbery and a plastic component, the density of IPNs should increase due to any interpenetration of the chains and specific volume contributions [22,23]. In this case, the experiment values of density were obviously higher than that from additivity rule for the UB films. This indicated that a strong intermolecular interaction occurred between PU and B-KGM, which suggests that B-KGM molecules penetrated into PU networks to bind intimately with PU, therefore, led to a reduction of the free volume of original PU.

DMF is good solvent of B-KGM, while the PU network is basically insoluble in this case. Thus using DMF to extract B-KGM from the UB films, the miscibility information between PU and B-KGM can be obtained. The B-KGM amount extracted with DMF as a function of B-KGM

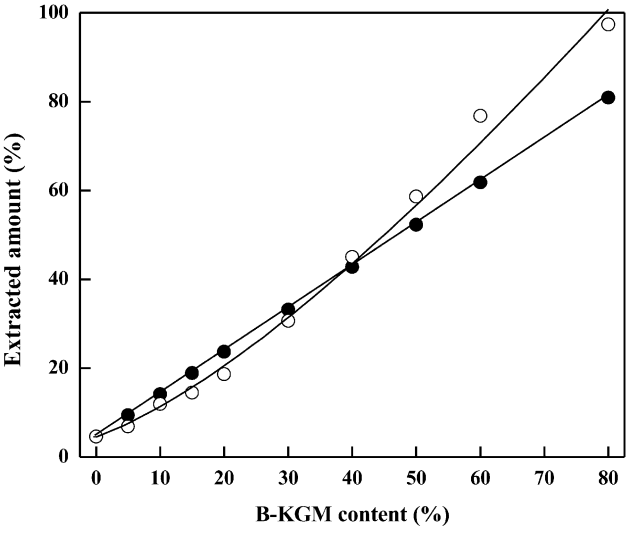

Fig. 4. Dependence of the theoretical (●) and experimental (○) amounts of B-KGM extracted with DMF from the UB films on original B-KGM content.

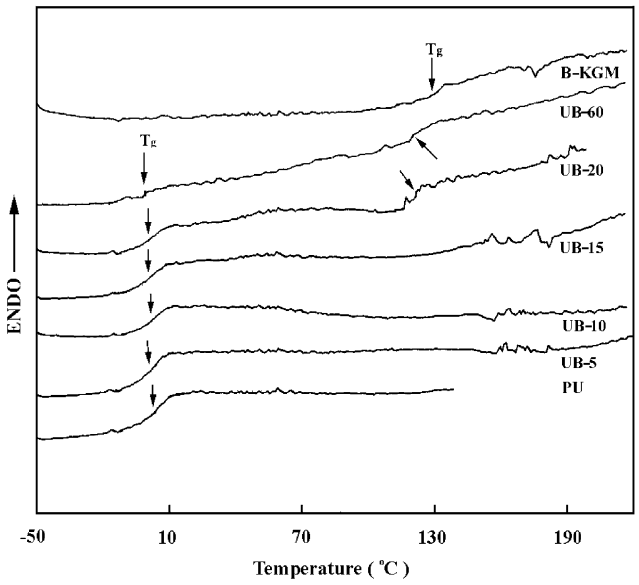

Fig. 5. The DSC thermograms of the films PU, B-KGM and UB.

content for the UB films is shown in Fig. 4. The extracted B-KGM amount was higher than the expected values for the films UB-50, UB-60, UB-70 and UB-80. This implies that a small quantity of PU was removed, because the DMF is a good solvent for both linear B-KGM and uncross-linked PU. When B-KGM content was more than 40 wt%, the extracted B-KGM amounts of the UB films were higher than the theoretical values, indicating that excessive amount of B-KGM hindered the PU network formation, and therefore increased the dissolution of B-KGM and uncross-linked PU molecules, similar to the semi-IPNs based on PU/polydimethylsiloxane reported by Yu et al. [21]. Interestingly, when B-KGM content in the UB films was less than 40 wt%, the extracted B-KGM amounts were lower than the theoretical values. This implies that the strong molecular bind and entanglement between B-KGM and PU networks impeded the dissolution of B-KGM from PU networks, similar to poly(vinyl chloride) and oligomeric MDI isocyanate cross-linked networks reported by Pittman Jr et al. [24].

DSC thermograms and the corresponding data of the UB films with various B-KGM content are shown in Fig. 5 and Table 1, respectively. The T_g of PU film was observed in about −3.6 °C, and that of B-KGM was located at 124 °C. A single glass transition region was observed for films from UB-5 to UB-15, implying a good miscibility caused by mixing on molecular level between PU and B-KGM. However, when B-KGM content was more than 20 wt%, the UB films exhibited two T_g transition regions, which shifted to the lower temperature comparing with that of individual component, but the T_g of both PU and B-KGM shifted toward each other. It indicated an occurrence of a certain degree of phase separation between PU and B-KGM, namely semi-miscible polymer pairs [16]. The T_g values for the UB films were even lower than that of pure PU networks. This can be explained that an effect of linear

Table 1
The thermal data from DMA and DSC for the films PU, B-KGM and UB

Films	DMA		DSC			
	T_{g1} (°C)	T_{g2} (°C)	T_{g1} (°C)	ΔC_{p1} (J g^{-1} °C^{-1})	T_{g2} (°C)	ΔC_{p2} (J g^{-1} °C^{-1})
PU	25		− 3.6	0.357		
UB-5	–		− 5.9	0.354		
UB-10	–		− 6.2	0.333		
UB-15	23		− 5.6	0.281		
UB-20	19	121	− 6.3	0.341	115	0.259
UB-40	14	135	–	–	–	–
UB-60	5	156	− 3.8	0.125	117	0.249
UB-80	2	157	–	–	–	–
B-KGM		163			124	0.224

B-KGM molecules enhanced flexibility and mobility of the PU soft segment phase and reduced the crystallization of PU due to the incorporation of B-KGM [25], resulting in the reduction of T_g and the heating capacity change (ΔC_p) [26].

The DMA spectra of the films are shown in Figs. 6 and 7, and the corresponding data are summarized in Table 1. The storage modulus of the UB films with B-KGM content lower than 15 wt% showed a drop in stiffness, accompanying the tan δ transition of PU soft domains. As B-KGM content increased, the UB films exhibited two transitions corresponding to each component. The loss peak is associated with the glass transition, and its height and shape provide information about the degree of order and freedom of molecular mobility of soft segments [27]. There was one loss peak for the UB films having low B-KGM content (<20 wt%), implying good miscibility between PU and B-KGM. However, when B-KGM content in the UB films was higher than 20 wt%, two loss peaks corresponding to each component were observed for the UB films. Moreover, the tan δ peaks of both PU and B-KGM for the films from UB-60 to UB-20 shifted toward each other, indicating that the UB films are miscible to some degree. This is in good agreement with the results from DSC and SEM. The broad prominent damping peaks corresponding to the B-KGM in the UB films reflect the toughness and multi-molecular motion of the polymer materials. In addition, the crystallization behavior of the polymers can be described by the shape of the tan δ peak [27]. The prominent damping peaks in the films UB-20 to UB-80 suggested an enhancement of amorphous. Fig. 8 shows the WAXD patterns of the films. The diffraction peak for the UB films broadened with the increase of B-KGM content, which indicates that the crystallization of PU in the semi-IPN became progressively difficult, therefore, supported the conclusions from DSC and DMA.

3.2. Morphology of the UB films

The SEM photographs of the UB films extracted with DMF are shown in Fig. 9. The fractured sections of UB-10, UB-30, UB-40 and UB-50 all exhibited homogeneous porous architecture, indicating a good or certain level miscibility between B-KGM and PU. The white domain represents the PU networks, and the dark domain is the void, where the B-KGM molecules were removed. When B-KGM content in the UB films was lower than 40 wt%,

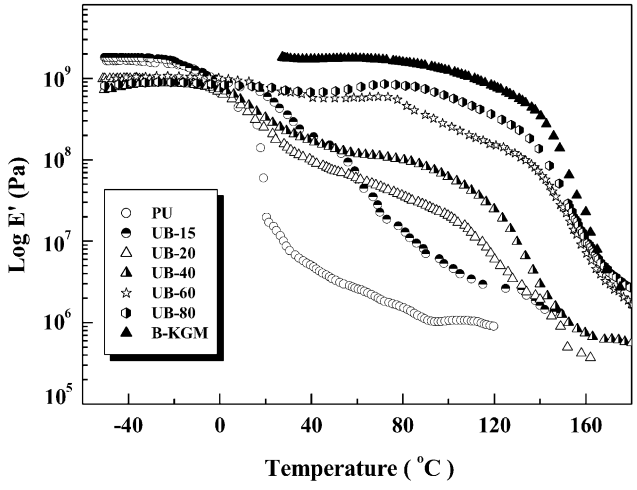

Fig. 6. Temperature dependence of storage modulus (log E') for the films PU, B-KGM and UB.

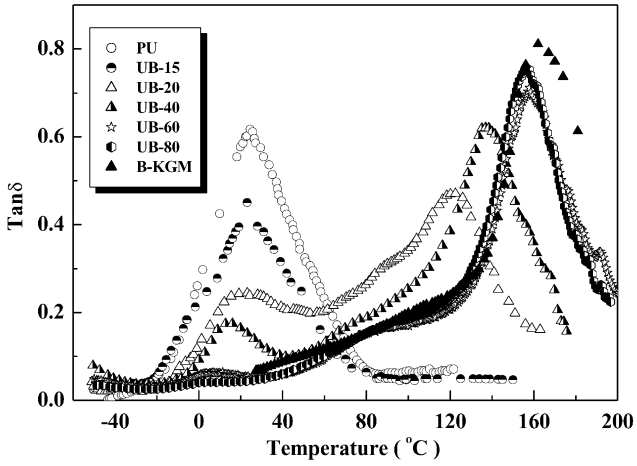

Fig. 7. Temperature dependence of tan δ for films PU, B-KGM and UB.

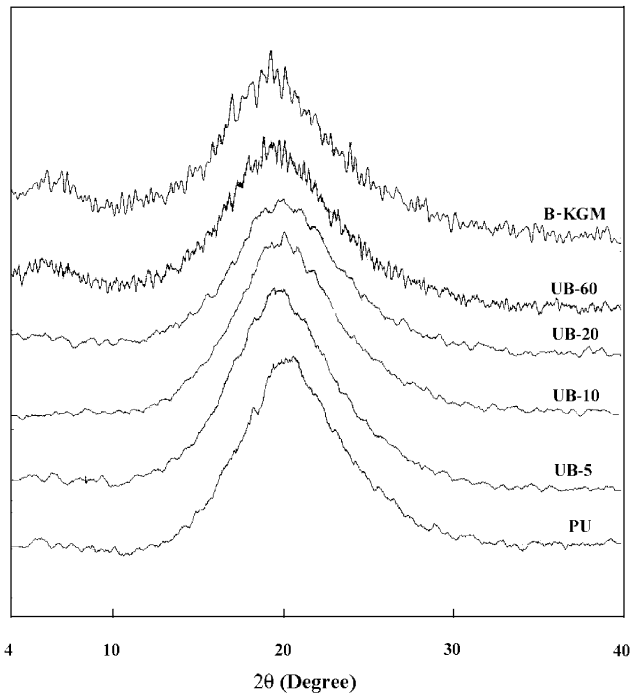

Fig. 8. The WAXD patterns of the films PU, B-KGM and UB.

PU formed a continuous phase and B-KGM as a dispersed phase. With an increasing amount of B-KGM, the dark phase became more dominant. At the 50 wt% B-KGM content in the UB films, dual-phase continuity was observed, suggesting taking place of phase inversion between two polymers. The SEM photographs of the UB films with B-KGM content more than 60 wt% could not be obtained due to difficult preparation of samples. General trends toward PU matrix with dispersed B-KGM domains of 30–300 nm for the UB-10 films, 200–2000 nm for the UB-30 and 500–5000 nm for the UB-40 films were observed. Therefore, this work provided a novel method to characterize the morphology and its transition of the semi-IPNs by extracting the soluble linear polymer from the PU networks.

On the basis of the results obtained from DSC, DMA and SEM, a continuous phase and dual-continuous phase model describing the semi-IPNs from PU and B-KGM are shown in Fig. 10. B-KGM molecules penetrated into the PU networks and formed a dispersed phase, when B-KGM content was relatively low. With an increase of B-KGM content in the UB films, the B-KGM phase domain size gradually grew up to achieve the dual-phase continuity. As B-KGM content further increased, a small amount of PU network still existed, which dispersed into the B-KGM continuous phase.

3.3. Properties of the UB films

The transparency of the films is an auxiliary criterion to judge the miscibility of the composite materials [28]. The B-KGM content dependence of light transmittance (T_r) for the UB films is shown in Fig. 11. Interestingly, the UB films with B-KGM content lower than 20 wt% exhibited higher T_r of 95–80% than the PU film (79%), suggesting better miscibility and stronger interaction between B-KGM and PU. Enhanced T_r of the films can be explained that adhesion between two kinds of the molecules with small dispersed phase domain was very intimate, and the amorphous state enhanced, due to the IPN structure. Therefore, the higher T_r may be correlative with the amorphous state, phase domain, interfacial interaction and the match in refractive indices of two polymers. A similar phenomenon has been reported for PU/polyacrylate IPN [29]. However, the films UB-30 to UB-80 exhibited relatively low T_r. When B-KGM content was higher than 20 wt%, the certain degree of phase

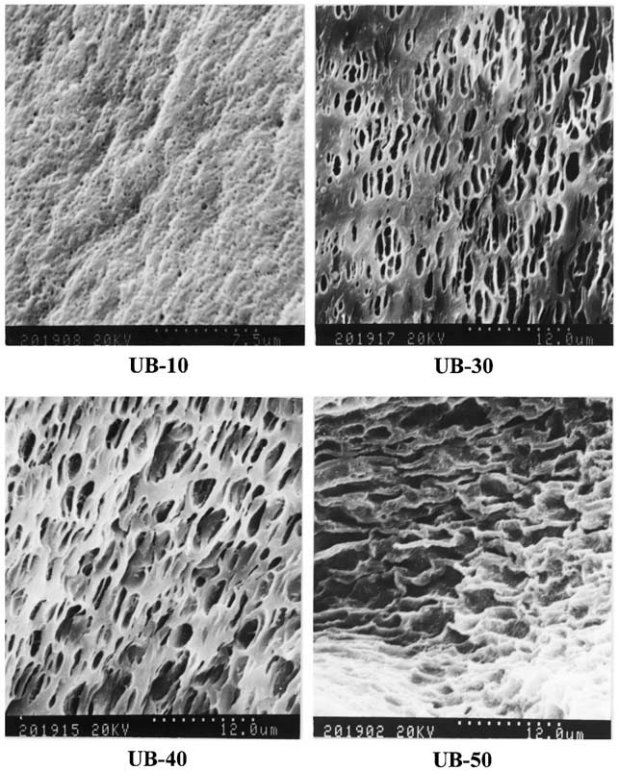

Fig. 9. The SEM photographs of the fracture section for UB films extracted with DMF.

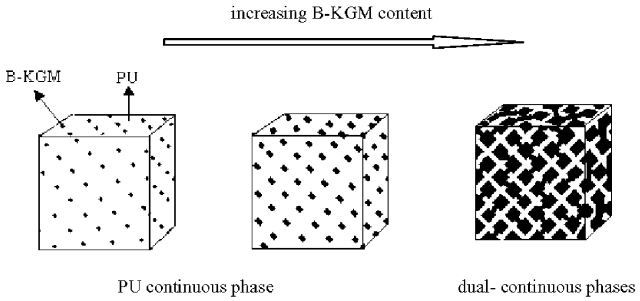

Fig. 10. Schematic diagrams of continuous phase and dual-continuous phase describing the semi-IPN from PU (white) and B-KGM (dark).

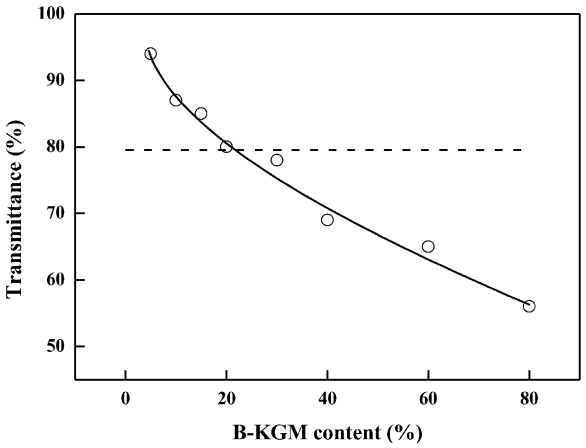

Fig. 11. The B-KGM content dependence of light transmittance at 800 nm for the UB films. Mark (- - -) represents film PU.

separation between PU and B-KGM in the UB films occurred, resulting in the loss of the light transmittance.

The stress–strain curves for the films PU, B-KGM, UB are given in Fig. 12. The tensile strength (σ_b) of the UB films increased from 7 to 45 MPa, and the breaking elongation (ε_b) decreased from 250 to 18% with an increase of B-KGM content from 0 to 80 wt%. It is worth noting that the UB films with relatively low B-KGM content displayed clearly elastomeric behavior. However, a yield point for UB-80 film was observed, indicating a plastic character. The area under the stress–strain curve can be used as a measurement of the material toughness. The relatively large area of the films UB-40 to UB-80 indicated a character of toughened plastic. Usually, the combination of rubbery and plastic polymers gives a blend materials changed from reinforced elastomers to rubbery-toughened plastics. The morphological transition from PU continuous phase to predominated B-KGM phase determined the mechanical properties of the films from UB-5 to UB-80. This is well consistent with the changes of dynamic storage modulus shown in Fig. 6. An increase in B-KGM content was accompanied by an increase in storage modulus for the UB films. The B-KGM films exhibited the highest storage modulus, and the storage modulus of the UB films increased with increase of B-KGM content, implying the effective reinforcement of PU matrix with B-KGM molecules.

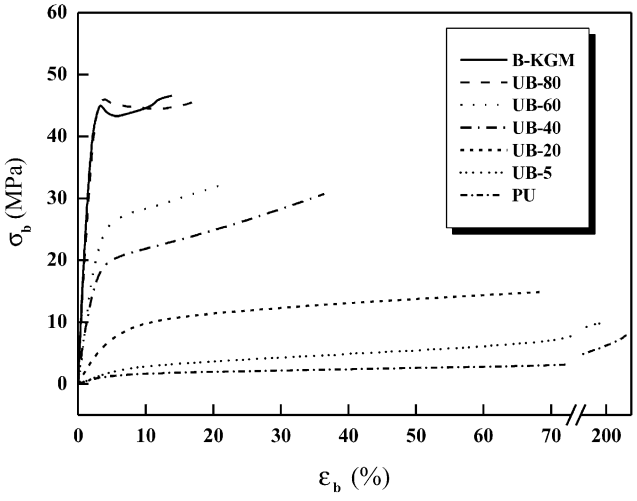

Fig. 12. The stress–strain curves for the films PU, B-KGM and UB.

4. Conclusions

Semi-IPN films were successfully prepared from castor oil-based PU and linear B-KGM with content from 0 to 80 wt%. The semi-IPN UB films were good or semi-miscible over the entire composition range. The morphology and properties of the UB films depended significantly on the B-KGM content. The UB films with B-KGM content lower than 15 wt% was good miscible and had relatively high density, good light transmittance and high breaking elongation. The certain degree of phase separation between PU and B-KGM was observed for UB films with B-KGM content more than 20 wt%. The tensile strength of the UB films increased from 7 to 45 MPa with an increase of B-KGM content from 0 to 80 wt%. The UB films behaved as reinforced elastomers at relatively low B-KGM content, and as toughened plastics at B-KGM content higher than 40 wt%, depending on the continuous phase and phase domain size. The continuous phase and dual-continuous phase models describing the semi-IPNs were proposed to illustrate the morphology and its transition. By extracting the B-KGM with DMF from the semi-IPNs, the morphology of the UB films was clearly observed by SEM. The B-KGM phase domain size dispersed in PU continuous phase grew up with an increase of B-KGM content till to reach a dual-continuous phase state, and then become a B-KGM continuous phase.

Acknowledgements

This work was supported by Major Grant of the National Natural Science Foundation of China (59933070), Major Grant of Science and Technology Project from Hubei Province and the Laboratory of Cellulose and Lignocellulosic Chemistry of The Chinese Academy of Sciences.

References

[1] Vogl O, Jaycox GD. Prog Polym Sci 1999;24:3.
[2] Takahadhi R, Kuskabe I, Kusama S, Sakurai Y, Murakami K, Mackawa A, Suzuki T. Agric Biol Chem 1984;48:2943.
[3] Ridout MJ, Brownsey J, Morris VJ. Macromolecules 1998;31:2539.
[4] Gao S, Zhang L. Macromolecules 2001;34:2202.
[5] Lu Y, Zhang L. Ind Engng Chem Res 2002;41:1234.
[6] Yue CL, Davé V, Kaplan DL, McCathy SP. Polym Prepr 1995;36:416.
[7] Brannon PL, Reilly Williama JJ. Proc Int Symp Control Rel Biact Biomater 1996;23:497.

[8] Sperling LH. Interpenetrating polymer networks and related materials. New York: Plenum Press, 1981.
[9] Hourston DJ, Schäfer FU. J Appl Polym Sci 1996;62:2025.
[10] Hsieh KH, Liao DC, Chen CY, Chiu WY. Polym Adv Technol 1996;7:265.
[11] Lee DS, Kwan SK, Kim SC. In: Klempner D, Fridch KC, editors. Advances in interpenetrating polymer networks, vol. IV. Lancaster: Technomic, 1994. p. 213.
[12] Tsunoda S, Suzuki Y. In: Klempner D, Fridch KC, editors. Advances in interpenetrating polymer networks, vol. 2. Lancaster: Technomic, 1990. p. 177.
[13] Zhang L, Zhou Q. J Polym Sci: Polym Phys 1999;37:623.
[14] Liu H, Zhang L. J Appl Polym Sci 2001;82:3109.
[15] Zhang L, Zhou J, Huang J, Gong P, Zhou Q, Zheng L, Du Y. Ind Engng Chem Res 1999;38:4284.
[16] Hourston DJ, Schäfer F-U. Polymer 1996;37:3521.
[17] Sugiyama N, Shimahara H, Andoh T, Takemoto M, Kamata T. Agric Biol Chem 1972;36:1381.
[18] Devia N, Manson JA, Sperling LH, Conde A. Macromolecules 1979;12:360.
[19] Miller JA, Lin SB, Hwang KKS, Wu KS, Gibson PE, Cooper SL. Macromolecules 1985;18:32.
[20] Paik Sung CS, Smith TN, Sung NH. Macromolecules 1980;13:117.
[21] Xiao H, Ping ZH, Xie JW, Yu TY. J Polym Sci: Polym Chem 1990;28:585.
[22] Kim SC, Klempner D, Frisch KC, Frisch HL. Macromolecules 1976;9:258 see also p. 263.
[23] Mathew AP, Packirisamy S, Thomas S. J Appl Polym Sci 2000;78:2327.
[24] Pittman Jr CU, Xu X, Wang L, Toghiani H. Polymer 2001;41:5405.
[25] Mishra V, Du Prez F, Sperling LH. J Polym Mater Sci Engng 1995;72:124.
[26] Cuve L, Pascault JP. Polymer 1992;33:3957.
[27] Son TW, Lee DW, Lim SK. Polym J 1999;31:563.
[28] Krause S. J Macromol Sci: Rev Macromol Chem 1972;7:251.
[29] Yang J, Winnik MA, Ylitalo D, DeVoe RJ. Macromolecules 1996;29:7047.